Competition between Energy and Dynamics in Memory Formation

Chloe W. Lindeman,* Varda F. Hagh,† Chi Ian Ip, and Sidney R. Nagel
Department of Physics and The James Franck and Enrico Fermi Institutes The University of Chicago, Chicago, Illinois 60637, USA

(Received 31 October 2022; revised 10 March 2023; accepted 19 April 2023; published 12 May 2023)

Bistable objects that are pushed between states by an external field are often used as a simple model to study memory formation in disordered materials. Such systems, called hysterons, are typically treated quasistatically. Here, we generalize hysterons to explore the effect of dynamics in a simple spring system with tunable bistability and study how the system chooses a minimum. Changing the timescale of the forcing allows the system to transition between a situation where its fate is determined by following the local energy minimum to one where it is trapped in a shallow well determined by the path taken through configuration space. Oscillatory forcing can lead to transients lasting many cycles, a behavior not possible for a single quasistatic hysteron.

DOI: 10.1103/PhysRevLett.130.197201

The ability of a physical system to store information about how it was prepared—memory—is now recognized as being crucial for the behavior of a large variety of disordered materials [1]. Jammed packings of soft spheres subjected to repeated cycles of shear, cyclically crumpled sheets of paper, and interacting spins in an oscillating magnetic field all form memories of how they were trained [2–12]. Memory in such systems hinges on the ability to learn a pathway between metastable states of the energy landscape. It has been compared to the memory seen in a collection of bistable elements, called hysterons, that flip between states when an external field is varied above or below a critical value [13–16]. Although an enormous simplification, ensembles of independent hysterons capture surprisingly well some features of the memory formation seen in complex systems [1,15,17,18].

However, independent hysterons fail to capture other features that are often seen [15,19–21]. For example, the configuration produced at the end of the first cycle is guaranteed to be the same as that found after subsequent cycles of the same amplitude. This is the case because each hysteron separately has this property. By contrast, cyclically sheared packings can take many cycles to train and can exhibit a multiperiod response [22] in which the periodicity of the response is an integer multiple of the driving period as first demonstrated in systems with friction [23]. Recent work has shown that generalizing the simple idea of a hysteron as an independent two-state object by adding interactions can result in long training times and multiperiod responses [16,19,20].

Here, we generalize the behavior of hysterons in a different way: by studying the effect of dynamics. Starting from a two-spring configuration that gives rise to a symmetric double-well potential, we add features one at a time to uncover the criteria for landing in one basin or the other. When a symmetry-breaking third spring is added, the behavior is determined by a competition between the timescale of applied forcing and the timescale of inherent system dynamics that relaxes the system to lower energy. There is a crossover, depending on deformation velocity, between energy-dominated and path-dominated selection criteria. Following from this, for oscillatory driving we find a critical frequency that separates the two regimes. Finally, we characterize the effect of allowing the system to age by slowly evolving the spring stiffnesses.

Bistable systems such as the ones we analyze here have previously been studied in the context of spin systems in an external field [24,25], in optical switches [26,27], and in bistable electronic circuits [27,28], and the importance of dynamics in hysteresis has been applied to systems as complex as allosteric proteins [29]. In many cases, the goal was to compute dissipation in the system undergoing oscillatory forcing [24–26,30,31]. Other studies have characterized the response of systems to a forcing that varies in time [32,33], often focusing on the effects of stochastic noise. Here, we approach this hysteretic behavior from a memory-formation perspective.

In two dimensions, two identical harmonic springs with rest lengths ℓ_0 and stiffnesses k_0 connected by a single node produce a bistable system as shown in Figs. 1(a) and 1(b). ϵ is the distance of each outer node from its "rest-length" position where the two outer nodes are exactly a distance $2\ell_0$ apart. The central-node location is the only variable since the positions of the two outer nodes are

explicitly controlled. We study the behavior of this system with overdamped dynamics, where the total force f_T from all springs on the middle node is proportional to its velocity v_m: $f_T = \beta v_m$. We choose the units of length, force, and time to be ℓ_0, $k_0\ell_0$, and β/k_0, respectively. With these units, the relation between velocity and force is $v_m = f_T$.

The energy is the sum of the spring energies,

$$E = \left(\sqrt{x^2 + (1-\epsilon)^2} - 1\right)^2,$$

which, to first order in ϵ and fourth order in x, is

$$E \approx \frac{1}{4}x^4 - \epsilon x^2. \tag{1}$$

As in a Landau expansion, the sign of ϵ determines whether one or two minima exist. As seen in Fig. 1(a), when $\epsilon > 0$, corresponding to a bistable, buckled configuration, the quartic and quadratic terms have opposite signs, and the energy is a double well. For $\epsilon < 0$, the springs are stretched, and there is only one minimum.

We drive the dynamics by forcing the outer nodes to move with some velocity $\vec{v}_o$. We restrict the motion of those nodes to be symmetric about the x axis so that the middle-node trajectory is one dimensional (in x) and any $v_{o,y}$ enters the equations only as a time-dependent ϵ. We can account for the remaining motion of the outer nodes $v_{o,x}$ by choosing a reference frame in which the outer nodes are stationary in the x direction. The effect of using a moving frame is that the middle node moves with respect to $x = 0$ with an additional velocity: $\Delta v_m = -v_{o,x}$. This movement is *in addition* to the velocity caused by the springs themselves. With overdamped dynamics, this can be treated as an additional force, $-v_{o,x}$, in the x direction. The resulting effective energy can then be written as

$$E_{v_x} \approx \left(\frac{1}{4}x^4 - \epsilon x^2\right) + v_{o,x}x. \tag{2}$$

The symmetry of the two-spring system can also be broken by attaching a third, weak spring to the middle node so that it applies an additional force along the x axis, as shown in Fig. 1(c). If the other end of the third spring is pinned such that the equilibrium position is far away, the force will be approximately independent of the position, and the modified energy will be given by

$$E \approx \left(\frac{1}{4}x^4 - \epsilon x^2\right) - f_w x, \tag{3}$$

where f_w is the small force due to the weak spring. The form of this equation is identical to that of Eq. (2), so we can include any outer-node motion in the x direction to produce an effective force: $f_{\text{eff}} \equiv f_w - v_{o,x}$.

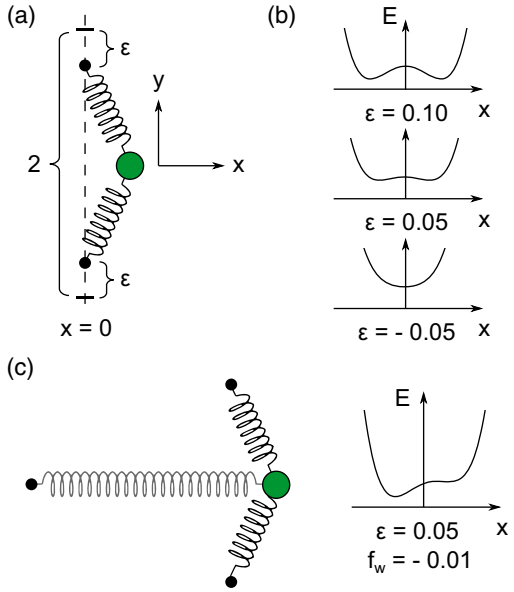

FIG. 1. (a) Schematic of the two-spring system. Outer nodes are shown as black dots. Middle node is shown as a green circle. (b) Energy versus position of the middle node. For large ϵ, the two wells are deep and well separated. As ϵ decreases, the wells become smaller and the minima move closer together; they coalesce as $\epsilon \to 0$. For $\epsilon \leq 0$, there is only one minimum. (c) Three-spring system with $f_w \neq 0$ showing energy versus middle-node position. In the energy diagram, the force is pulling to the left (in the negative x direction).

This model of a hysteron thus has two distinct mechanisms that compete to determine f_{eff}. If f_{eff} is dominated by the weak spring, then the behavior will be "energy dominated," with the *true* landscape changing slowly enough that the energetics determine which well is chosen. If, on the other hand, the velocity of the outer nodes dominates, then the behavior will be "path dominated": the energy landscape will change too quickly for the system to keep up with the local minimum and so it will become trapped in a state determined by the path of the boundaries (and hence the *effective* energy).

We probe the transition from one to two minima by starting the middle node at $x = 0$ and bringing the two outer nodes together at a constant velocity $\vec{v}_o$. Starting from the stretched state with one minimum, ϵ changes from negative to positive as the two nodes approach one another, causing the initial minimum to separate into two. If $v_{o,x} = 0$ and $f_w = 0$, the energy landscape remains perfectly symmetric and the system chooses a minimum randomly (if there is any noise) or remains stuck in the unstable equilibrium position $x = 0$. For nonzero $v_{o,x}$ and f_w, we can find the critical $v_{o,x}$ that leads to $f_{\text{eff}} = f_w - v_{o,x} = 0$. For $v_{o,x} < f_w$, the system is energy-dominated and ends up in the global minimum; for $v_{o,x} > f_w$, the system is path-dominated and becomes trapped in the shallower (less-favorable) minimum.

We connect this three-spring system to conventional hysteron models by fixing the two outer nodes and oscillating the free end of the weak spring at frequency, ω, to modulate the weak force:

$$f_w(t) = f_0 + A\sin(\omega t). \tag{4}$$

Regardless of the oscillation frequency, ω, the system will be trapped forever if both wells are stable at all times; likewise, it will fall to the global minimum if one well is never stable. We therefore focus on an intermediate case where the time-averaged landscape ($f_w = f_0$) is stable but one well disappears for a fraction of each cycle.

We study the dynamics numerically by starting the middle node in the less-favorable well and calculating the net force on (and hence the velocity of) the middle node and updating its position accordingly. For low ω, the system finds the lower well quickly; for high ω, the system never finds the lower well. At intermediate frequencies, there is a regime where the system displays surprising complexity. As shown in Fig. 2(a), the middle node can appear to be trapped for some time in the less-favorable well but continue to creep toward, and finally fall into, the global minimum. As ω increases, the escape time to reach the lower well, τ_e, increases until the system becomes permanently trapped in the local minimum. As shown in the inset to Fig. 2(a), the time for the node to escape to the global minimum diverges as $\tau_e \propto (\omega_c - \omega)^{-1/2}$.

Similar behavior was studied numerically and experimentally in optical bistable devices [27]. It was shown there that the critical frequency ω_c scales as A, the amplitude of forcing. We find the scaling of ω_c around the critical behavior for all system variables analytically using an argument quite different from the calculations in [27]. Even during times in the cycle when one minimum has disappeared, the motion will be limited by the bottleneck where the force, and hence velocity, is smallest. There is a "saddle-node remnant," where two zeros of the force (corresponding to the less-favorable well and energy maximum) merge and disappear; this dominates the dynamics [34]. Getting through this region is therefore the limiting factor in escaping to the global minimum. At any frequency, the net motion over one cycle will be exactly zero in the infinite-time limit when the system has reached a periodic orbit. For a system near the critical frequency, this net motion is centered on the bottleneck. We find ω_c by calculating the frequency at which the motion in one half of the cycle is exactly undone by the motion in the other half:

$$\omega_c \sim \frac{|A|\epsilon^{1/4}}{(f_0 + 2(\frac{2}{3}\epsilon)^{3/2})^{1/2}}. \tag{5}$$

See [35] for detailed calculation.

Existence of a critical frequency indicates that the behavior of a dynamic hysteron is determined by a competition between the timescale of external driving, set by ω, and the time it takes to travel a given distance, set by the net force from the springs at any given moment. Any process that alters one of these timescales can therefore change the behavior of the system.

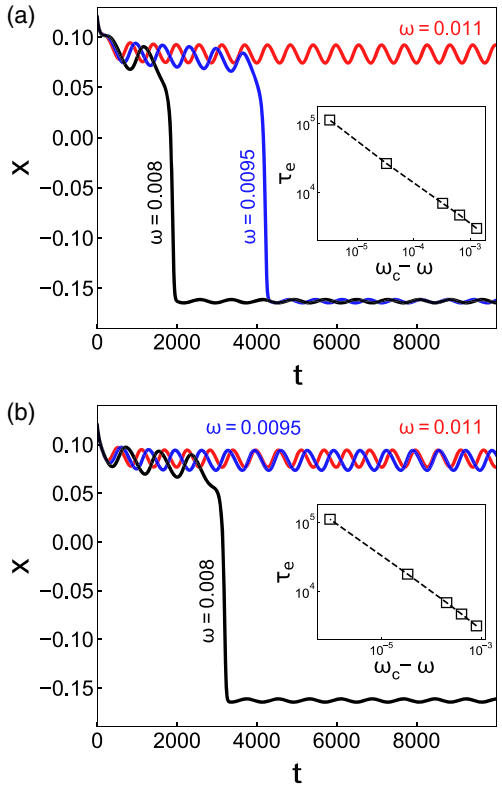

FIG. 2. (a) Position versus time for a single dynamical hysteron driven at different frequencies. We have used $\epsilon = 0.01$, $A = -10^{-4}$, and $f_0 = -0.00108$, and have set the initial middle-node position to be $x = 0.12$. The black and blue curves take multiple cycles before falling into the global minimum; the red curve is above the critical frequency, $\omega_c \approx 0.0103$, at which the escape time diverges and the system thus remains in the less-favorable (upper) well. (b) Trajectories of the same system driven with similar fixed amplitude and values of the driving frequencies after the system has been aged. Now only the black curve falls into the global minimum because the critical frequency has decreased to $\omega_c \approx 0.0088$. Both insets indicate the divergence of escape time, τ_e, with slope $= -0.50$ as ω approaches ω_c.

One example of such a process is "directed aging" in which local properties of a spring network, such as the spring constants or bond lengths, evolve in response to the stresses imposed on each bond [36–38]. This leads to changes in the global elastic response of the system.

In these dynamic hysterons, each spring, i, undergoes a strain $\delta\ell_i$ when the system is driven. We evolve the spring constants, k_i, at a rate proportional to the energy stored in each bond with proportionality constant q:

$$\frac{dk_i(t)}{dt} = -qk_i(t)\delta\ell_i^2. \tag{6}$$

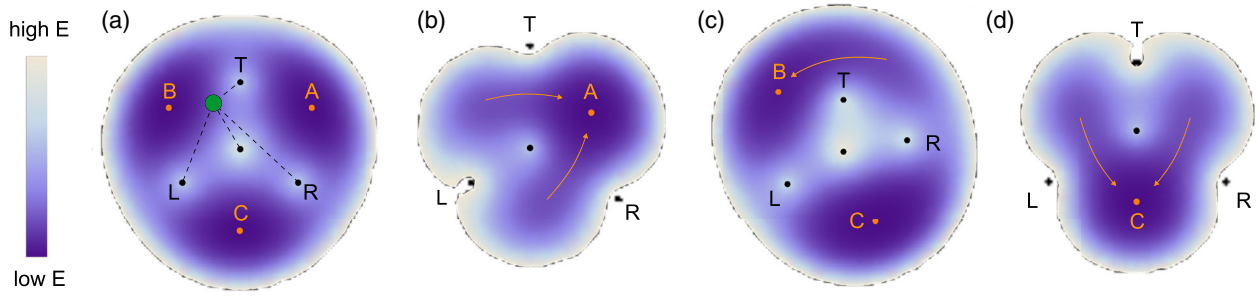

FIG. 3. (a) Energy landscape for a four-spring, three-well system. Black dots indicate the controlled boundary nodes L (left), R (right), T (top), and center; orange dots mark the resulting energy minima. Manipulating the boundary nodes forces some minima to disappear. (b) Moving T and R away from the center causes wells B and C to disappear and flow into A. (c) Moving T toward the center while moving R azimuthally causes well A to disappear and flow into B. (d) Moving L and R away from the center causes wells A and B to disappear and flow into C.

Figure 2(b) shows the trajectories for the same systems and frequencies depicted in Fig. 2(a) after the system is aged. Starting with $k_{s0} = 1$ in the strong springs and $k_{w0} = 10^{-3}$ in the weak spring, we update the stiffness values according to Eq. (6) with $q = 5 \times 10^{-5}$. During aging, each individual spring is held at the fixed value of strain it undergoes when $x = 0.12$. For the weak spring, the aging strain is fixed at $\delta\ell_w = |f_0 + A|/k_w$ where $\delta\ell_w \gg \delta\ell_s$ for the strong springs, which leads to much faster aging in the weak spring. After aging the system for $t = 50$, we fix the spring constants at their aged values and drive the system as in Fig. 2(a). Because the critical frequency is shifted to a lower value, the middle node can only fall into the global minimum for the lowest frequency shown. It is also possible to increase the critical frequency by aging the system in ways that slow down the dynamics.

Hysterons with more than two wells can also be constructed in a network of springs as shown, for example, in the three-well system in Fig. 3. The presence of a third well allows for behavior not possible in a bistable system. For example, if the three wells are designated A, B, and C, by prescribing the motion of the outer nodes T, L, and R, one can create a reversible boundary motion that causes the middle node to transition from A → B → C → A over the course of a single full cycle. This can be achieved using two types of outer node motion: one in which two nodes are pulled away from the center, causing the two opposite wells to disappear, and one in which one node is brought toward the center and another is moved azimuthally so that one well (e.g., C) remains unaffected and the others flow (e.g., A → B). See [35] for cycle details and a video of the corresponding energy landscape. The node's trajectory is topologically nontrivial, a feature that may be important in systems like jammed packings that are sheared cyclically but where the phase-space trajectory typically forms complex loops.

Systems with three rearrangements per cycle are not new: this behavior is possible with pairs of quasistatic hysterons and is typically associated with an avalanche (see [35]). However, just as our generalization of hysterons from quasistatic to dynamic allowed us to see multicycle transient behavior previously found in hysteron systems only when interactions were present, generalizing from two to three wells has allowed us to see three rearrangements arising from a different, geometric mechanism. It is an interesting question whether there is a fundamental, measurable difference between an avalanche-driven three-rearrangement cycle and one which is geometrically created.

We have introduced a model that generalizes the notion of hysterons to a dynamical unit that exhibits a variety of distinct behaviors in response to driving. Starting with two springs connected to an overdamped node, we show that the system's path is the only factor that determines which well it will choose. Adding a weak spring breaks the symmetry and brings in the energy landscape as another way to determine which minimum is chosen. Thus there is a competition between energy and path for choosing the minimum. For cyclic driving, the system can require multiple cycles to reach its global minimum.

The model presented is suitable for studying the effect of dynamics in cyclically driven experimental systems where a frequency-dependent behavior is observed. In addition, the sensitivity of the model to directed aging shows its versatility and opens the door to a large variety of training possibilities, for example, in mechanical preconditioning of soft tissues [39,40]. One natural generalization of this model would be to include interactions between pairs of dynamical hysterons. In the case of ordinary (quasistatic) hysterons, the presence of interactions leads to memories that include multiple cycles [16,19,20]. It would be interesting to see if unexpected behavior emerges by allowing interactions between pairs of dynamical hysterons.

The system presented here is simple enough to be studied analytically, yet has dynamics that are rich with complexity. The examples above illustrate that it is easily adaptable to a variety of systems, i.e., where interactions between hysterons play a role, or more complex scenarios

as in the case of a three-well system. This dynamical hysteron model can thus provide insight into the effect of new timescales on a wide variety of complex systems.

We thank Peter Littlewood, Arvind Murugan, and Cheyne Weis for useful conversations. This work was supported by the NSF MRSEC program NSF-DMR 2011854 (for model development) and by the US Department of Energy, Office of Science, Basic Energy Sciences, under Grant DE-SC0020972 (for the analysis of aging phenomena in the context of memory formation). C. W. L. was supported by a NSF Graduate Research Fellowship under Grant DGE-1746045. C. I. I. was supported by the Center for Hierarchical Materials Design (70NANB14H012).

C. W. L. and V. F. H. contributed equally to this work.

*cwlindeman@uchicago.edu
†vardahagh@uchicago.edu

[1] N. C. Keim, J. D. Paulsen, Z. Zeravcic, S. Sastry, and S. R. Nagel, Rev. Mod. Phys. **91**, 035002 (2019).
[2] L. Corte, P. M. Chaikin, J. P. Gollub, and D. J. Pine, Nat. Phys. **4**, 420 (2008).
[3] D. Fiocco, G. Foffi, and S. Sastry, Phys. Rev. Lett. **112**, 025702 (2014).
[4] D. Fiocco, G. Foffi, and S. Sastry, J. Phys. Condens. Matter **27**, 194130 (2015).
[5] M. Adhikari and S. Sastry, Eur. Phys. J. E **41**, 1 (2018).
[6] F. Arceri, E. I. Corwin, and V. F. Hagh, Phys. Rev. E **104**, 044907 (2021).
[7] P. Charbonneau and P. K. Morse, Phys. Rev. Lett. **126**, 088001 (2021).
[8] K. Matan, R. B. Williams, T. A. Witten, and S. R. Nagel, Phys. Rev. Lett. **88**, 076101 (2002).
[9] D. Shohat, D. Hexner, and Y. Lahini, Proc. Natl. Acad. Sci. U.S.A. **119**, e2200028119 (2022).
[10] A. Szulc, M. Mungan, and I. Regev, J. Chem. Phys. **156**, 164506 (2022).
[11] C. Merrigan, D. Shohat, C. Sirote, Y. Lahini, C. Nisoli, and Y. Shokef, arXiv:2204.04000.
[12] D. Shohat and Y. Lahini, Phys. Rev. Lett. **130**, 048202 (2023).
[13] F. Preisach, Z. Phys. **94**, 277 (1935).
[14] N. C. Keim, J. Hass, B. Kroger, and D. Wieker, Phys. Rev. Res. **2**, 012004(R) (2020).
[15] M. Mungan, S. Sastry, K. Dahmen, and I. Regev, Phys. Rev. Lett. **123**, 178002 (2019).
[16] M. van Hecke, Phys. Rev. E **104**, 054608 (2021).
[17] M. Mungan and T. A. Witten, Phys. Rev. E **99**, 052132 (2019).
[18] T. Jules, A. Reid, K. E. Daniels, M. Mungan, and F. Lechenault, Phys. Rev. Res. **4**, 013128 (2022).
[19] C. W. Lindeman and S. R. Nagel, Sci. Adv. **7**, eabg7133 (2021).
[20] N. C. Keim and J. D. Paulsen, Sci. Adv. **7**, eabg7685 (2021).
[21] H. Bense and M. van Hecke, Proc. Natl. Acad. Sci. U.S.A. **118**, e2111436118 (2021).
[22] M. O. Lavrentovich, A. J. Liu, and S. R. Nagel, Phys. Rev. E **96**, 020101(R) (2017).
[23] J. R. Royer and P. M. Chaikin, Proc. Natl. Acad. Sci. U.S.A. **112**, 49 (2015).
[24] M. Rao, H. Krishnamurthy, and R. Pandit, J. Phys. Condens. Matter **1**, 9061 (1989).
[25] M. Rao, H. R. Krishnamurthy, and R. Pandit, Phys. Rev. B **42**, 856 (1990).
[26] P. Jung, G. Gray, R. Roy, and P. Mandel, Phys. Rev. Lett. **65**, 1873 (1990).
[27] C. Boden, F. Mitschke, and P. Mandel, Opt. Commun. **76**, 178 (1990).
[28] F. Mitschke, C. Boden, W. Lange, and P. Mandel, Opt. Commun. **71**, 385 (1989).
[29] I. Graham and T. A. J. Duke, Phys. Rev. E **71**, 061923 (2005).
[30] G. Bertotti, J. Appl. Phys. **69**, 4608 (1991).
[31] F. Broner, G. H. Goldsztein, and S. H. Strogatz, SIAM J. Appl. Math. **57**, 1163 (1997).
[32] M. C. Mahato and S. R. Shenoy, Physica (Amsterdam) **186A**, 220 (1992).
[33] M. C. Mahato and A. Jayannavar, Physica (Amsterdam) **248A**, 138 (1998).
[34] S. H. Strogatz, *Nonlinear Dynamics and Chaos: With Applications to Physics, Biology, Chemistry, and Engineering* (Addison-Wesley, Reading, MA, 1994).
[35] See Supplemental Material at http://link.aps.org/supplemental/10.1103/PhysRevLett.130.197201 for a detailed calculation of the critical frequency and example boundary motion that gives rise to chiral behavior in a three-well system.
[36] N. Pashine, D. Hexner, A. J. Liu, and S. R. Nagel, Sci. Adv. **5**, eaax4215 (2019).
[37] D. Hexner, A. J. Liu, and S. R. Nagel, Proc. Natl. Acad. Sci. U.S.A. **117**, 31690 (2020).
[38] D. Hexner, N. Pashine, A. J. Liu, and S. R. Nagel, Phys. Rev. Res. **2**, 043231 (2020).
[39] D. G. Moon, G. Christ, J. D. Stitzel, A. Atala, and J. J. Yoo, Tissue Eng. Part A **14**, 473 (2008).
[40] S. Majumdar, L. C. Foucard, A. J. Levine, and M. L. Gardel, Soft Matter **14**, 2052 (2018).